

Investigating the magnetic interaction with Geomag and Tracker Video Analysis: static equilibrium and anharmonic dynamics

This article has been downloaded from IOPscience. Please scroll down to see the full text article.

2012 Eur. J. Phys. 33 385

(<http://iopscience.iop.org/0143-0807/33/2/385>)

View [the table of contents for this issue](#), or go to the [journal homepage](#) for more

Download details:

IP Address: 137.112.34.173

The article was downloaded on 18/11/2012 at 21:21

Please note that [terms and conditions apply](#).

Investigating the magnetic interaction with Geomag and Tracker Video Analysis: static equilibrium and anharmonic dynamics

P Onorato, P Mascheretti and A DeAmbrosio

Department of Physics 'A Volta', University of Pavia, Via Bassi 6, I-27100 Pavia, Italy

E-mail: pasquale.onorato@unipv.it and anna.deambrosio@unipv.it

Received 25 November 2011, in final form 20 December 2011

Published 7 February 2012

Online at stacks.iop.org/EJP/33/385

Abstract

In this paper, we describe how simple experiments realizable by using easily found and low-cost materials allow students to explore quantitatively the magnetic interaction thanks to the help of an Open Source Physics tool, the Tracker Video Analysis software. The static equilibrium of a 'column' of permanent magnets is carefully investigated by working on digital photos, while the anharmonic oscillations of a magnetic bar under the action of gravity and of magnetic repulsion are analysed by using a digital video. A detailed comparison between theoretical expectations and experimental results is discussed. We discuss how the magnetic force falls off with the distance between the permanent magnets following an inverse p th power law. Static and dynamic measurements of the force and of the periods for small amplitude harmonic oscillations yield an experimental value for $p \approx 2$. The dynamical system is a good example of an anharmonic oscillator. The experiments need simple and inexpensive material to be realized and address a relevant topic in the physics curriculum; thus, they appear appropriate to be used in high school and undergraduate physics courses.

(Some figures may appear in colour only in the online journal)

1. Introduction

In this paper, we present two experiments aimed at exploring quantitatively the magnetic interaction by using low-cost material improved by new technologies.

Our choice was to integrate the use of a popular toy, the Geomag magnetic building kit [1], very effective for investigating force between magnetic bars [2, 3], with the Tracker Video Analysis and Modeling Tool (TVA). TVA is an Open Source Physics (OSP) tool, built on

the OSP code library [4] and included in the ComPADRE Digital Library [5], that allows students to dynamically model and analyse the motion of objects in videos. By overlaying the dynamical models directly onto videos, students may see how well a model matches the real world.

In the paper, a detailed comparison between the results of the experiments and theoretical models of magnetic interaction is carried out in order to find out how the magnetic force falls off with the distance between two permanent magnets.

In section 2, magnetic dipole interaction is briefly discussed and the hypothesis that the magnetic force falls off with the distance between the magnets according to an inverse power law, $\vec{F}_M(d) = \hat{r} \frac{A_M}{r^p}$, is introduced.

The first experiment, described in section 3, is aimed at measuring the magnetic dipole–dipole interaction under static conditions by considering a column of 12 interacting magnets in a glass tube in equilibrium.

The second experiment focuses on the periodic motion of an oscillating system consisting of a magnetic bar falling in a glass tube, which is pushed back by another magnetic bar fixed at the bottom of the tube. The experiment shows how the TVA is suited both for measuring the force as a function of the distance between the permanent magnets and for investigating harmonic and anharmonic oscillations. In section 4.1, we discuss the direct measurements of the force and we obtain an estimation of the magnitude of the magnetic repulsion as a function of the end-to-end distance between the magnetic bars. The exponent p can be measured both from the fit of the force for unitary mass versus distance and from the measurements of the equilibrium point. In section 4.2, the exponent p is estimated by means of the value of the period of the falling magnet motion measured for small oscillation amplitudes. In section 4.3, the dependence of the period on the amplitude of oscillation is studied to focus on the passage from the harmonic to the anharmonic phase of motion.

2. Magnetic dipole interaction

Calculating the attractive or repulsive force between two magnets is, in the general case, a complex operation, since it depends on the shape, magnetization, orientation and separation of the magnets. However, an analytical expression was proposed in [6] for describing the attraction force between two cylindrical permanent magnets on the assumption of uniform magnetization. Although the assumption was not fulfilled exactly, the authors obtained very good agreement between the calculated and measured forces. Thus, for two identical cylindrical magnets with radius R and height h , with their axes aligned, the force can be well approximated (if the cylindrical magnets are far from each other at least as the radius of the magnet) by

$$F \propto \frac{1}{r^2} + \frac{1}{(r+2h)^2} - \frac{2}{(r+h)^2}, \quad (1a)$$

where r is the separation between the two magnets.

This relation can be compared with the force between two electric dipoles, where the first term of equation (1a) corresponds to the interaction between the nearest poles (++) in figure 1(B)), the second term corresponds to the force between the distant poles (–– in figure 1(B)) and the third to the force between different poles. (+– in figure 1(B)).

However, for $r > h$, equation (1a) becomes

$$F \propto \frac{1}{r^4}. \quad (1b)$$

Equation (1b) represents the dipole–dipole interaction between two magnetic dipoles (the so-called dipole approximation) [7, 8]. On the other hand, when the distance between the two

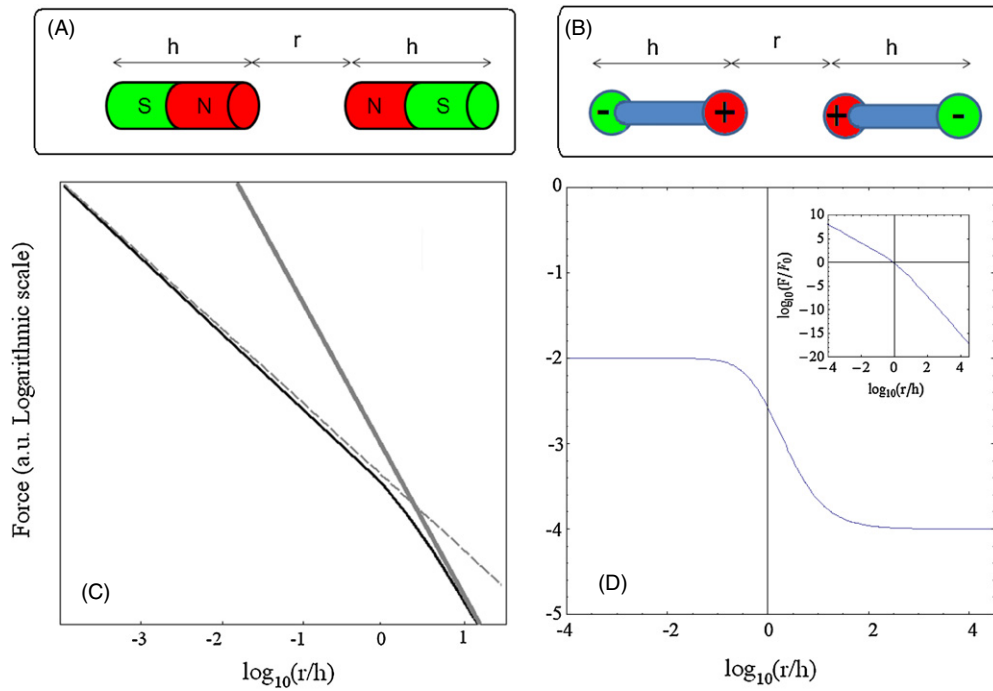


Figure 1. (A) Schematic of the interacting magnetic bars. (B) Schematic of two interacting electric dipoles. (C) Log–log plot of the force versus distance given by equation (1a) (black line) compared with the two limit cases of small (grey dashed line equation (1c)) and large distances (grey thick line equation (1b)). (D) The exponent (slope of the plot in panel C) corresponding to a power law describing locally the magnetic force in equation (1a).

interacting bar magnets is much smaller than their length ($r < h$), according to equation (1a), the interaction force is approximately proportional to the inverse of the distance squared:

$$F \propto \frac{1}{r^2}. \quad (1c)$$

In figure 1, the force given by equation (1a) is plotted and compared with the two limit cases of small and large distances.

Based on these results, we assume that the force falls off with the distance between the permanent magnets according to an inverse power law,

$$\vec{F}_M(d) = \hat{r} \frac{A_M}{r^p}, \quad (2)$$

and we estimate p by means of different experiments.

Figures 1(C) and (D) allow us to compare the plot of the force versus distance corresponding to equation (1a) with the limit cases of small and large distances. From this, an estimate of the error induced by approximating the force with a $\frac{1}{r^4}$ law or with a $\frac{1}{r^2}$ law can be obtained.

3. Static measurements

Many experiments have been proposed to measure dipole–dipole magnetic interaction. In some of them, magnets supported by a meter-stick balance are employed [9, 10], while in

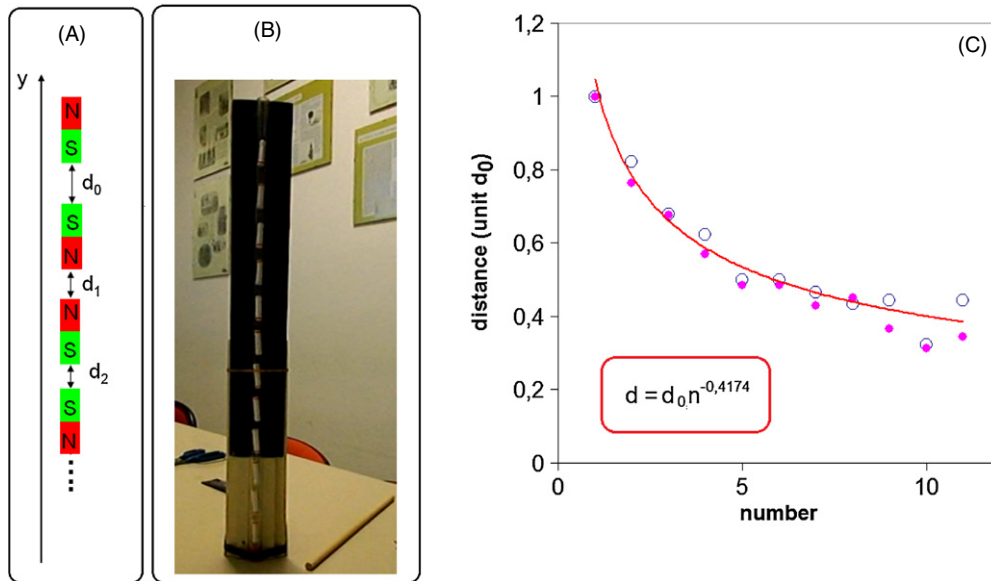


Figure 2. (A) The repelling configuration for the 12 Geomags in a vertical glass tube (outer diameter 12 mm). (B) Digital photo of the system. Geomag bar magnets are 6 mm in diameter and 30 mm in length ($h = 0.03$ m), completely covered in hard plastic except at their two ends. (C) Plot of the measured distances versus the number, counting the bar magnets from the top. Two different sets of data (filled-empty dots) and the fitting power law function (continuous line) are reported.

others, magnets are placed in a glass tube [11]. In all these experiments, a magnetic force in the form of equation (2) with $p = 2$ was found, corresponding to the inverse square law interaction of equation (1c).

3.1. The experiment

Twelve identical¹ Geomag bar magnets (radius $R = 3$ mm, length 30 mm) are placed end to end in a vertical glass tube (diameter 12 mm) in a repelling configuration, as reported in figure 2(A). Starting from a photo as that reported in figure 2(B) acquired by means of a digital CCD camera, we measure, with the help of the digital photo analysis, the positions y_i of the ends of each magnetic bar. Then the separation between two adjacent magnets is obtained from top to bottom. The largest distance between two Geomags is between the highest pair where $d_0 \approx 21.3$ mm.

In figure 2(C), the measured distances d_n are reported as a function of the number of magnets n , counting from the top. Data show a power law decay of d_n . The interpretation of these results by means of a theoretical nearest-neighbour model allows us to find the exponent p of the power law describing the magnetic interaction (see equation (2)), as explained in the following section.

¹ The variation in the magnetic dipole momentum of the sample of Geomags used is below 7%, according our measurements

3.2. Experimental data and nearest-neighbour model

3.2.1. Model. We start from the hypothesis that the magnitude of the magnetic force falls off with the distance d between the opposite poles following an inverse p th power law as in equation (2). We apply a nearest-neighbour model, often used in statistical and condensed matter physics, i.e. we suppose that each Geomag interacts just with the upper and lower bar magnets. It follows that, if the distance between the highest magnet in the column and its first neighbour is d_0 , the total force on the highest magnet is

$$M\vec{g} + \hat{y} \frac{A_M}{d_0^p} = 0, \quad (3)$$

where M is the mass of the Geomag bar and A_M is a constant including the magnetic momentum of the permanent magnets. It follows that

$$d_0 = \left[\frac{A_M}{Mg} \right]^{1/p}. \quad (4)$$

The equation of the steady state for the n th magnet is

$$M\vec{g} + \hat{y} \left(\frac{A_M}{d_n^p} - \frac{A_M}{d_{n-1}^p} \right) = 0. \quad (5a)$$

This corresponds to

$$d_n = d_{n-1} d_0 \left[\frac{1}{d_{n-1}^p + d_0^p} \right]^{1/p}. \quad (6)$$

We can solve analytically equation (6) by using the hypothesis

$$d_n = d_0 n^\alpha. \quad (7)$$

Then we find α by substituting equation (7) into equation (6). It shows that the distance follows the power law with an exponent

$$\alpha = -1/p. \quad (8)$$

Once we have found α with the nearest-neighbour approximation, we are able to estimate the error δ_n induced on d_n by neglecting the second nearest neighbour. It can be done by modifying equation (5a) with the addition of two terms,

$$M\vec{g} + \hat{y} \left(\frac{A_M}{d_n^p} - \frac{A_M}{d_{n-1}^p} \right) - \hat{y} \left(\frac{A_M}{[d_n + d_{n+1} + h]^p} - \frac{A_M}{[d_{n-1} + d_{n-2} + h]^p} \right) = 0. \quad (5b)$$

It follows that $\delta_n \propto n^{-1}$ and $\delta_n/d_n \leq 6\%$ for p between 2 and 2.5, and δ_n/d_n negligible for large n .

3.2.2. Results. The experimental data, reported in figure 2(C), show that the distance d_n follows a power law with an exponent $\alpha = 0.42 \pm 0.04$ according to equation (7). Then an estimated value for the power law exponent p in equation (2) is

$$p = 2.4 \pm 0.2.$$

With reference to figure 1, we can see that in our experiment $\log_{10}(r/h)$ is in the range -1 to 0. Then p is expected to have a value between 2 and 2.5.

This result is in agreement with the idea that, if we consider the bar magnets as dipoles, the influence of the far poles may be neglected when the distance between the magnets is smaller than their length ($d_n < h$). In this case, the interaction force is inversely proportional to the squared distance.

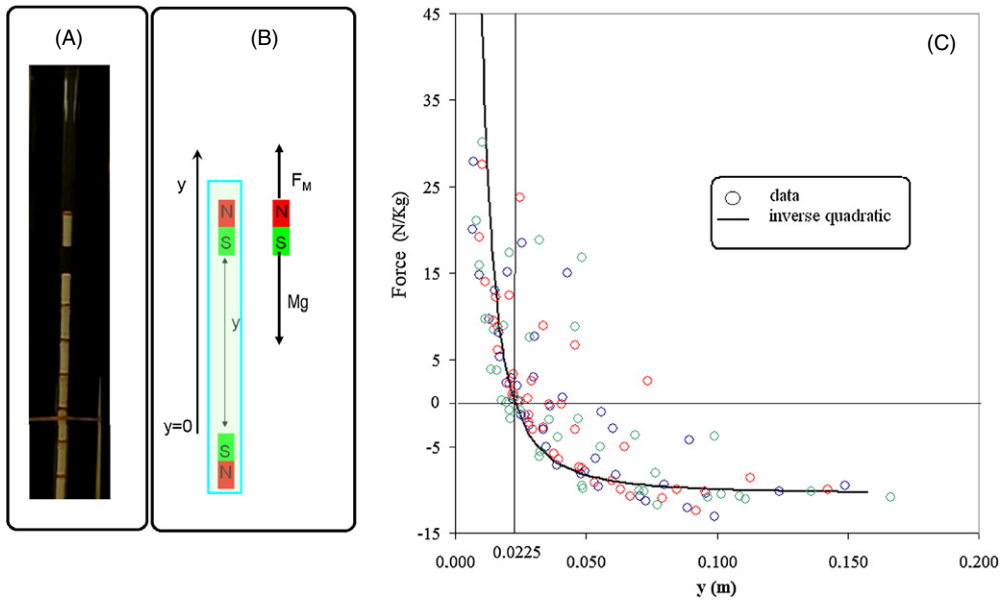


Figure 3. (A) Experimental configuration of the magnetic bouncing Geomag oscillator. (B) Schematic of the system. (C) The measured force for unitary mass (acceleration) versus the end–end distance from the bottom magnetic pole. A strongly nonlinear behaviour is clearly shown and a fitting line $F \propto 1/y^2$ is shown. Data from three different runs are plotted.

4. Dynamical measurements

4.1. The experiment

The idea of using the oscillations of a magnet in a magnetic field in order to measure the magnetic interaction and evaluating the dependence of the force on the distance between the interacting magnetic dipoles is not new [12]. For our experiment, we used the same equipment described in figure 2(A), but now a Geomag is placed at the bottom of the glass tube, while one (or two) Geomag is allowed to fall from the top in the repelling configuration (figure 3(B)). The motion of the Geomag is registered by a digital camera and a video is obtained. The measurements were carried out by acquiring the position versus time values, thanks to the TVA software, for a set of oscillations of the system (attained with a frequency, frame s^{-1} , of 30 Hz).

Data were acquired for several runs also by changing the mass of the falling bar (M or $2M$).

In figure 3, the experimental setup of the magnetic bouncing Geomag oscillator (A) and a corresponding sketch of the experiment (B) are reported for a single oscillating magnetic bar. In panel (C), the force (for unitary mass) evaluated by means of position versus time data is represented as a function of position.

4.2. Evaluating p from force measurements

4.2.1. Model. The measured force $F_r(y)$ in figure 3(C) shows a strongly nonlinear behaviour. According to the hypothesis that the magnitude of the magnetic force depends on the distance

between the magnets, as described by equation (2), the force $F_r(y)$ acting on the falling magnet can be written as

$$F_r(y) = -Mg + \frac{A_M}{y^p}, \quad (9)$$

assuming as $y = 0$ the top end position of the repelling magnet (see the inset in figure 3(A)).

We can calculate y_{eq} , the equilibrium position where the sum of the acting forces vanishes: $y_{\text{eq}} = \left(\frac{A_M}{Mg}\right)^{-1/p}$. Since y_{eq} depends on the mass as $M^{-1/p}$, when we consider two Geomag bars falling in the tube, we obtain $y_{\text{eq}}(2M) = (2)^{-1/p} d_0$, while $y_{\text{eq}}(M) \equiv d_0$. Thus, from the measured values of the equilibrium points, we can obtain a value for p as

$$p = \left(\log_2 \left[\frac{y_{\text{eq}}(M)}{y_{\text{eq}}(2M)} \right] \right)^{-1}. \quad (10)$$

4.2.2. Results. The experimental data for a falling magnet reported in figure 3(C) show good agreement with the curve describing a force inversely proportional to the distance squared. However, in order to obtain a quantitative estimation of p , we can consider the measured equilibrium points for a double Geomag system. The experimental value of y_{eq} for a single Geomag is $y_{\text{eq}}(M) = 22.5 \pm 0.5$ mm (see figure 3(C)), in agreement with the result obtained statically in section 2. From the data of $F_r(y)$ for two falling magnetic bars, $y_{\text{eq}}(2M) = 15.5 \pm 0.5$ mm was measured.

According to equation (10), we can calculate

$$p = 1.9 \pm 0.3$$

in agreement with $p \approx 2$, true when the distance between two aligned Geomags is smaller than their length.

4.3. Evaluating p from the period in the harmonic approximation

4.3.1. Model. Figure 4(A) shows the position versus time for two runs of a bar magnet oscillating in the glass tube. In figure 4(B), $y(t)$ for two runs of two oscillating magnets is reported.

Both the systems are anharmonic since, as discussed in section 3.2, the force is strongly nonlinear; then the period depends on the amplitude of the oscillations. However, for oscillations with small amplitude around y_{eq} , we can expand the force as

$$F_r(y) \approx F_r(y_{\text{eq}}) + \kappa(y - y_{\text{eq}}) + \kappa_2(y - y_{\text{eq}})^2 + \dots, \quad (11a)$$

and approximate as

$$F_r(y) \approx F_r(y_{\text{eq}}) + \kappa(y - y_{\text{eq}}), \quad (11b)$$

where $F_r(y_{\text{eq}}) = 0$ and

$$\kappa = \left[-p \frac{A_M}{y^{p+1}} \right]_{y=y_{\text{eq}}} = p \frac{Mg}{y_{\text{eq}}} = p \frac{(Mg)^{\frac{p+1}{p}}}{A_M^{1/p}}. \quad (12)$$

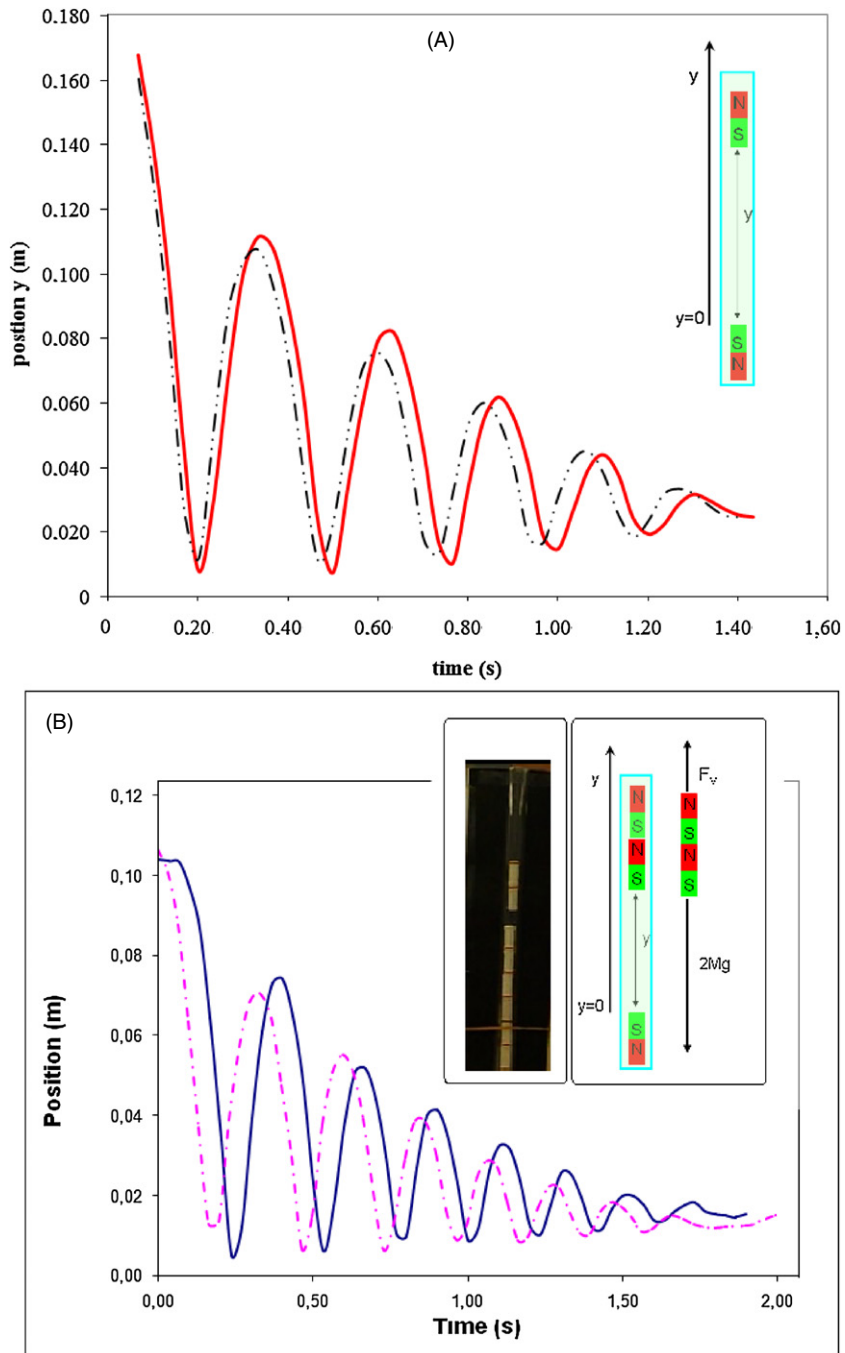


Figure 4. (A) Time dependence of the position versus time for one bouncing Geomag (A) and for two bouncing Geomags (B). In the insets of (B), the experimental configuration of the two magnetic bouncing Geomag oscillators and schematic of the experiment are shown.

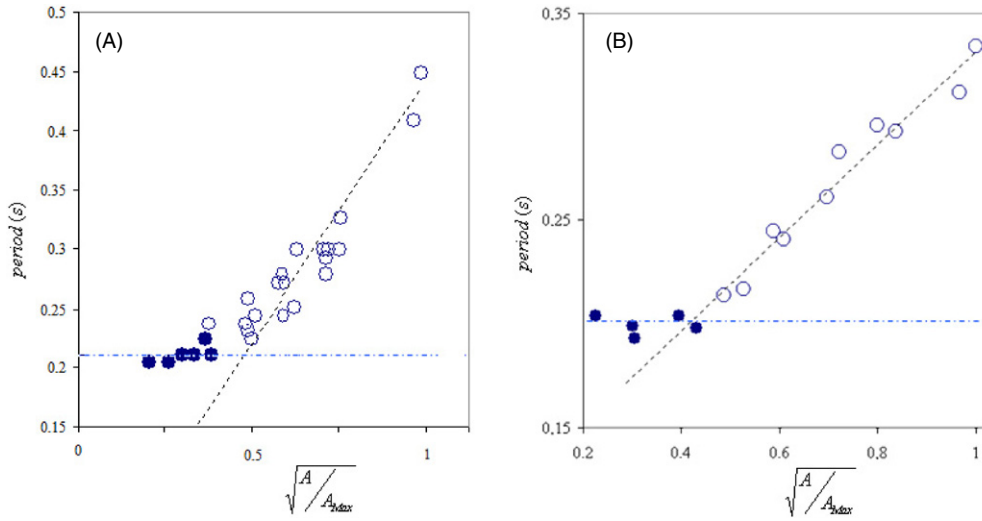


Figure 5. Period of the Geomag oscillations as a function of the square root of amplitude (normalized to the maximum value A_{Max}) for one (A) and two (B) oscillating magnets. Open dots: first phase of the motion. Full dots: second phase (harmonic motion). A fitting line is also drawn for the anharmonic phase. The maximum amplitude, A_{Max} , is ≈ 16 cm for one and ≈ 9 cm for two oscillating magnets.

4.3.2. Results. The experimental value $y_{\text{eq}}(M) = 22.5 \pm 0.5$ mm can be used to evaluate $\kappa/M \approx p \times 435$ N Kg $^{-1}$, from equation (12). The period of small amplitude oscillations obtained from this value is

$$T = \frac{2\pi}{\omega} = 2\pi \sqrt{\frac{M}{k}} \approx \frac{0.30}{\sqrt{p}}. \quad (13)$$

From the data reported in figure 4(A), the period can be measured for small oscillation amplitudes. We obtain $T(M) \approx 0.21 \pm 0.01$ s, corresponding to

$$p = 2.0 \pm 0.1.$$

4.4. The anharmonic oscillations

The bouncing Geomag is an example of an anharmonic [13] one-dimensional oscillator, a type of system investigated in a number of papers [14–20]. Data acquired by means of the TVA software and used for the measurements described above allow us also to study the period of the oscillating magnet as a function of the amplitude (figure 5). The figure shows two phases in the oscillatory motion of the magnet: an anharmonic phase (open dots) where the period strongly depends on the amplitude and a harmonic phase (full dots) where the period is constant.

Data show a sharp passage from the anharmonic to the harmonic phase with the crossover localized around a value of $\sqrt{A_C/A_{\text{Max}}} \approx 0.4$ for both cases. This corresponds to $A_C \approx 25$ and $A_C \approx 15$ mm, for one or two oscillating Geomags respectively.

5. Conclusion

The dipole–dipole magnetic interaction, which rapidly decreases as the distance between the dipoles increases, was difficult to explore quantitatively in the past. However, measurements

of this interaction may now become a simple and amusing task thanks to the help of easily found and low-cost material (the little magnetic sticks of a popular toy) coupled with a digital camera and video analysis software like TVA.

The static equilibrium of a ‘column’ of permanent magnets piled up in a glass tube was investigated by working on digital photos. The detailed comparison between the experimental results and the model of magnetic force, falling off with the distance r between the permanent magnets according to a power law, $F_M \propto r^{-p}$, lets us evaluate the exponent p .

Next we described how our experimental setup is suited for investigating the force’s dependence on the distance between the magnets straightforwardly from the data acquired during the motion of a falling magnet repelled by a second magnet. The resulting measurement of p can be compared with the indirect evaluation of p coming from the data about the equilibrium position and the period of the harmonic oscillations. We concluded that

$$p = 2.1 \pm 0.3,$$

in agreement with the theoretical value when the distance between the poles of two interacting magnetic dipoles is smaller than their length.

We discussed also harmonic and anharmonic oscillations and we focussed on the presence of the ‘crossover amplitude’ of oscillation, which characterizes the transition from the harmonic to anharmonic regime.

Since the experiments require simple and inexpensive material to be implemented and address a basic issue in the physics curriculum, they seem suitable to be introduced in high school and undergraduate physics courses and can be presented with several variations by both changing the magnets and the geometry of the system.

References

- [1] www.geomagworld.com/
- [2] Bonanno A, Bozzo G, Camarca M and Sapia P 2009 Weighting magnetic interactions *Phys. Educ.* **40** 570–2
- [3] Bonanno A, Camarca M and Sapia P 2011 Magnetic interactions and the method of images: a wealth of educational suggestions *Eur. J. Phys.* **32** 849–66
- [4] Defrancesco S, Logiurato F and Karwasz G 2007 Geomag™ paradoxes *Phys. Teach.* **45** 431–4
- [5] www.compadre.org/osp/webdocs/Tools.cfm?t=Tracker
- [6] www.compadre.org/
- [7] Vokoun D, Beleggia M, Heller L and Sittner P 2009 Magnetostatic interactions and forces between cylindrical permanent magnets *J. Magn. Magn. Mater.* **321** 3758–63
- [8] Castaner R, Medina J M and Cuesta-Bolao M J 2006 The magnetic dipole interaction as measured by spring dynamometers *Am. J. Phys.* **74** 510–3
- [9] Kraftmakher Y 2007 Magnetic field of a dipole and the dipole–dipole interaction *Eur. J. Phys.* **28** 409
- [10] Lufburrow R A 1963 Inverse-square law experiment *Am. J. Phys.* **31** 60–2
- [11] Romer A 1973 Magnetic repulsion: an introductory experiment *Am. J. Phys.* **41** 1332–6
- [12] Defrancesco S and Zaneth V 1983 Experiments on magnetic repulsion *Am. J. Phys.* **51** 1023–5
- [13] Bisquert J, Hurtado E, Mafe S and Pina J 1990 Oscillations of a dipole in a magnetic field: an experiment *Am. J. Phys.* **58** 838–43
- [14] Fletcher N H 2002 Harmonic? Anharmonic? *Am. J. Phys.* **70** 12
- [15] Thomchick J and McKelvey J P 1978 Anharmonic vibrations of an ‘ideal’ Hooke’s law oscillator *Am. J. Phys.* **46** 40–5
- [16] Pecori B, Torzo G and Sconza A 1999 Harmonic and anharmonic oscillations investigated by using a microcomputer-based Atwood’s machine *Am. J. Phys.* **67** 228–35
- [17] Mohazzabi P 2004 Theory and examples of intrinsically nonlinear oscillators *Am. J. Phys.* **72** 492–8
- [18] Filipponi A and Cavicchia D R 2011 Anharmonic dynamics of a mass O-spring oscillator *Am. J. Phys.* **79** 7
- [19] Johannessen K 2011 An anharmonic solution to the equation of motion for the simple pendulum *Eur. J. Phys.* **32** 407–17
- [20] Lewowski T and Wozniak K 2002 The period of a pendulum at large amplitudes: a laboratory experiment *Eur. J. Phys.* **23** 461–4

-
- [19] Amore P and Fernández F M 2005 Exact and approximate expressions for the period of anharmonic oscillators *Eur. J. Phys.* **26** 589–601
Amore P, Fernández F M and Raya A 2005 Alternative perturbative approaches in classical mechanics *Eur. J. Phys.* **26** 1057–63
- [20] Rodríguez I and Brun J L 2000 A new method to compute the period of any anharmonic oscillator as a power series of the energy *Eur. J. Phys.* **21** 617